Journal of Materials Chemistry A

PAPER

Cite this: J. Mater. Chem. A, 2015, 3, 4687

Trifluoroacetylazobenzene for optical and electrochemical detection of amines†

Jhih-Fong Lin,[ab] Jarmo Kukkola,[a] Teemu Sipola,[a] Dilip Raut,[c] Ajaikumar Samikannu,[c] Jyri-Pekka Mikkola,[cd] Melinda Mohl,[a] Geza Toth,[a] Wei-Fang Su,[b] Tomi Laurila[e] and Krisztian Kordas*[a]

Received 8th October 2014
Accepted 16th January 2015

DOI: 10.1039/c4ta05358c

www.rsc.org/MaterialsA

In this work, we demonstrate the solution processing of optical and electrochemical dye sensors based on 4-(dioctylamino)-4′-(trifluoroacetyl)azobenzene and its application in sensing different amine compounds. Distinct optical response of the sensors exposed to ammonia, tetramethylammonium hydroxide, ethylamine, cadaverine and putrescine (typical compounds upon the decomposition of proteins) is observed. Incorporation of inkjet deposited thin films of the dye as sensors in food packages of ground meat and salmon is found as a feasible route to detect the appearance of biogenic amines produced by the degrading food products. Furthermore, we demonstrate an electrochemical amine sensor based on (trifluoroacetyl)azobenzene dye added in carbon nanotube–Nafion® composites. The electrochemical sensor exploits the reaction between the dye and amines to detect amines in electrolytes, while the carbon nanotubes provide large surface for adsorption and also provide a percolating electrical network for allowing efficient charge transfer at the electrode electrolyte interface.

1 Introduction

The demand for chemical sensors with sufficiently high resolution, selectivity and affordable cost to detect or even quantify common chemical compounds has fostered research in the field of household and food safety, healthcare as well as in homeland security. Different materials and fabrication processes have been developed to improve the detection limit for corresponding targets. Among these approaches, optical sensors represent a robust but simple methodology in sensing application, and typically exploit the change of optical absorption, direct fluorescence or Raman spectrum upon interaction/reaction with analytes (alcohols, amines, aldehydes, acids/bases).[1–3] For instance, sensors based on the change of optical absorbance in conjugated polymers (polythiophene derivatives) were applied to detect and discriminate volatile organic compounds,[4] and various kinds of diamines.[5] Supramolecular fibres made by electrospinning from polydiacetylene acid and polystyrene-*co*-poly(4-vinylpyridine) proved to be useful in colourimetric detection of organic amines.[6] Minute alteration of the refractive index of poly[methyl(3,3,3-trifluoropropyl)-siloxane] upon exposure to hydrocarbons was detected from human breath by applying the polymer on cleaved optical fibers.[7] Both colorimetric and luminescence detection was demonstrated to quantify hydrazine in various solutions having multiple analytes through the reaction between arylidenemalononitrile and the hydrazine.[8] A number of different organic molecules and inorganic–organic hybrid probes were shown as efficient and stable fluorescence based sensors for pH,[9] nitroaromatic explosives,[10] and diamines.[11] Surface plasmon resonant metal nanoparticles and thin films made of silver or gold that are applied on surfaces of prisms, waveguides and optical gratings have also been popular choices for discriminating and quantifying analytes during the past 20 years.[12]

Among the vast number of possible analytes, optical sensing of amines has been intensively studied because of its widespread utility in environmental,[13] drug/biotechnology[14,15] and food applications.[16,17] Recently, Mohr and co-workers have developed a series of trifluoroacetyl reactants for the colourimetric detection of analytes such as water vapor, alcohols, amines and thiols. The dye 4-(dioctylamino)-4′-(trifluoroacetyl)-azobenzene reacts with amines resulting in the blue shift of optical absorbance peak.[18–21] Being a strong electron acceptor, the trifluoroacetyl group of the dye in the presence of amines forms a hemiaminal group thus shortening the "box" of delocalized electrons which is limited to the diazobenzene

[a]Microelectronics and Materials Physics Laboratories, Department of Electrical Engineering, University of Oulu, P.O. Box 4500, FI-90570 Oulu, Finland. E-mail: lapy@ee.oulu.fi

[b]Department of Materials Science and Engineering, National Taiwan University, 1, Roosevelt Road, Section 4, Taipei 106-17, Taiwan

[c]Technical Chemistry, Department of Chemistry, Chemical-Biological Centre, Umeå University, SE-90187 Umeå, Sweden

[d]Industrial Chemistry & Reaction Engineering, Department of Chemical Engineering, Process Chemistry Centre, Åbo Akademi University, FI-20500, Åbo-Turku, Finland

[e]Department of Electrical Engineering and Automation, School of Electrical Engineering, Aalto University, 02150, Espoo, Finland

† Electronic supplementary information (ESI) available. See DOI: 10.1039/C4ta05358c

Scheme 1 Bonding reaction of 4-(dioctylamino)-4′-(trifluoroacetyl)azobenzene and amine.

backbone of the molecule in the product (Scheme 1).[18] Due to the stronger confinement, the resonance energy of the delocalized electrons increases and requires optical photons with shorter wavelength to induce excitation/absorption.

For demonstrating practical use, the dyes were incorporated plasticized poly(vinyl chloride)and applied in the form of membrane type films. The sensitivity of such optical sensors for amine detection was found to be influenced by the size, lipophilicity and the nucleophilic character of the amines.[18] To improve selectivity of the sensors towards aliphatic amines, the dyes were combined with cholesteric liquid crystals.[21]

More recently, the advancement of miniaturized electrochemical sensors such as low driving power and good selectivity/sensitivity have attracted attention in developing portable devices for sensing different biogenic amines in clinic medicine and food safety. Among those, sensing electrodes with carbonaceous nanomaterials such as carbon nanotubes (CNTs) and graphenes[22,23] are believed as the most potential candidates due to their high specific surface area, superior conductivity, and outstanding chemical stability. Chemical functionalization of the conductive surface with suitable receptor groups,[24–27] composites with polymers[28] and decoration with metal nanoparticles[29,30] are often applied to improve the key performance indicators thus opening newer horizons for practical applications.[23–25]

In this work, we are elaborating further on the exploitation of the (trifluoroacetyl)azobenzene dye to optically detect different types of amines in solutions and vapors using simple solution processed (*i.e.* spin coated or inkjet deposited) thin films of the dye. Response and recovery of the sensing films exposed to commonly appearing analytes such as ammonia, tetramethylammonium hydroxide, ethylamine, cadaverine and putrescine are studied. We are also evaluating the potential usability of the optical dye sensing films to be applied in food packages for monitoring the biogenic amines from degradation of meat and fish. In addition, we show dye–CNT–Nafion® composites on glassy carbon electrode as a feasible electrochemical sensor to detect amines.

2 Experimental

2.1 Chemicals

Ammonia (25%, Fluka), tetramethylammonium hydroxide (TMAH, 25 wt%, Sigma-Aldrich), ethylamine (66–72%, Aldrich), putrescine (99%, Aldrich), cadaverine (95%, Aldrich), tetrahydrofuran (99.8% LAB-SCAN), 2,3-butanediol (Fluka), 4-(dioctylamino)-4′-(trifluoroacetyl)azobenzene (>98%, Fluka), Nafion® (NR50, Aldrich), potassium chloride (KCl, ACS reagent, Sigma-Aldrich), carboxylic-functionalized single-walled carbon nanotube (4–5 nm × 500–1500 nm, Sigma-Aldrich). All the chemicals were received and used without further purification.

2.2 Sample preparation

Thin films of the dye for measuring absorption spectra were made by spin-coating (1000 rpm, 30 seconds) solutions of 4-(dioctylamino)-4′-(trifluoroacetyl)azobenzene in tetrahydrofuran (1 mg mL^{-1}) on cleaned polyethylene terephthalate foil (PET, thickness 125 μm, Melinex).

The sensors placed in the food packages were prepared by inkjet deposition using a materials printer (Dimatix DMP-2800, 10 pL nominal droplet volume, $T_{substrate} = 60$ °C, $T_{ink} = 55$ °C, $U_{piezo} = 20$ V). The inks were made by dissolving the dye in 2,3-butanediol (viscosity of ~7 cP) and then square-shaped patterns of 5 × 5 mm^2 size were printed (25 layers with 30 μm drop spacing) on polycrystalline alumina substrates. The nozzles of the cartridge are automatically cleaned between each printed layer.

The Nafion® solution was prepared by adding 40 mg Nafion® polymer to 40 mL ethanol/deionized water solution of 1 : 1 volumetric ratio and stirred at ~80 °C in a closed container. After for 4 hours, the dispersion was let cool to room temperature and stored for two days before collecting the supernatant fraction for further experiments. The dye–CNT–Nafion® composites for electrochemical sensors were prepared by dispersing 0.5 mg carboxyl functionalized CNTs in 1 mL of the prepared Nafion® solution using ultrasonic agitation and then mixing 1 mL of the 4-(dioctylamino)-4′-(trifluoroacetyl)-azobenzene dye solution (1 mg mL^{-1} in THF) while maintaining the ultrasonic treatment. The as obtained dispersion was then drop-cast on a cleaned glassy carbon electrode (GCE, 3 mm in diameter) to cover the rod until ~2 cm distance from its tip. The surface was dried under ambient condition. Three different amounts of the composite were deposited (20, 60 and 140 μL). The 20 μL sample was dispensed in a single shot on the surface and then dried under ambient conditions. In the case of the 60 μL and 140 μL samples, the deposition was carried out using ~20 μL aliquots dispensed with ~30 min drying periods before coating the next layer.

2.3 Characterization

Optical measurements. A commercially available organic dye, 4-(dioctylamino)-4′-(trifluoroacetyl)azobenzene was used as an optical and electrochemical probe molecule in the corresponding colourimetric and voltammetric measurements, respectively. In optical characterization, five different amines including ammonia, tetramethylammonium hydroxide (TMAH), ethylamine, putrescine, and cadaverine were applied

as analytes. The spectral change of absorbance after exposure to vapors and aqueous solutions of the amines were recorded as a function of analyte concentration as well as exposure and recovery times using a spectrophotometer (Cary 500-scan UV-Vis-NIR). To test alteration in the absorbance spectra of the sensors for detecting amines that evolve during the course of food degradation, sensor films spin-coated on PET were placed next to meat and fish and then the container was sealed for 90 hours. Note: due to the extended measurements periods, the calibration of the spectrophotometer drifted, thus the intensity of spectra showed minor shift as well. To eliminate this error, the spectra were manually reset to zero intensity at 800 nm wavelength.

Digital camera imaging and data processing. The measurements to visualize the color changes of the inkjet deposited dye films using a digital camera were conducted after 1 week storage of salmon fish and ground meat in the presence of the sensors. Reference color marks (red green and blue squares printed by a Canon iRC2620N Colour Photocopier on white Staples A4 copy paper, 80 g m^{-2}) were used for color calibration. The images of the sensor and the reference RGB patterns were taken by a photocamera (Panasonic Lumix DMC-LX7) under identical illumination conditions. For each sample, three pictures were taken before and after the exposure in the food package and processed *via* built-in transformation function of MATLAB to transfer the reference color and sensor patterns from RGB space to Lab space. The digitalization of color change was also defined as the distance between two vectors corresponding to the colors of reference sample and exposed dye sensor in Lab space respectively.

Electrochemical measurements. Cyclic voltammetry was performed in a standard three-electrode cell using a potentiostat (Princeton Applied Research VersaSTAT 3). The dye–CNT–Nafion® composite/GCE was used as the working electrode. Before depositing the composite film on the electrode, the surface was polished using a sandpaper (P1200, Mirka), and then sonicated in acetone, isopropanol and finally in deionized water for 10 minutes in each solvent. A platinum wire and silver chloride electrode (Ag/AgCl, Aldrich® glass reference electrode) were used as the counter and reference electrodes, respectively. All the electrochemical experiments were performed at room temperature using 50 mV s^{-1} sweeping rate. Before each experiment, the electrolyte was purged with N_2 for 30 minutes.

3 Results and discussion

3.1 Spectroscopy detection of amines using spin-coated and inkjet deposited dyes

As shown in Fig. 1(a), the absorption peak of the dye film is gradually shifting from 490 nm to 430 nm when placed in the vapor of 1% cadaverine solution. The blue-shift in the absorption spectra originates from the reaction between dye molecule 4-(dioctylamino)-4′-(trifluoroacetyl)azobenzene and the amine compound. In the structure of forming complex molecule, the

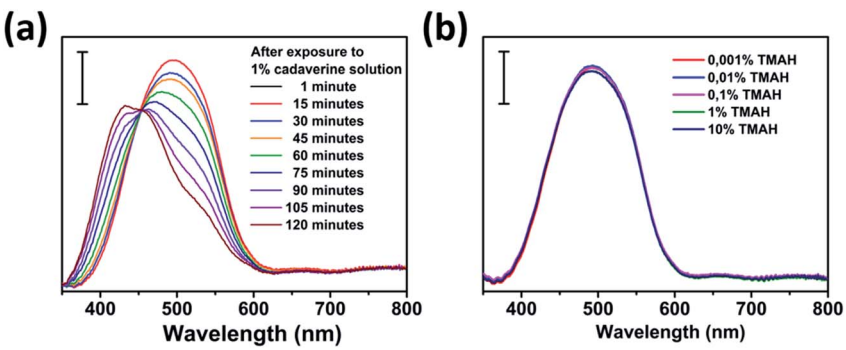

Fig. 1 Absorption spectra of spin-coated thin film dye sensors (a) in the course of 2 hours exposure to the vapor of 1% cadaverine solution and (b) after two hours of exposure to the vapors of TMAH solutions having different concentrations. Note: due to the drift of calibration in the long measurement periods, the plotted curves were manually shifted vertically to set the intensity values equal at 800 nm. The vertical bars show 5% optical absorption.

Table 1 Response of 4-(dioctylamino)-4′-(trifluoroacetyl)azobenzene films to amine vapors (+, blue shift; –, no visible change) and the reversibility of spectral change after removing the sensor from the corresponding vapor

Concentration of solution (vol%)	Ammonia	TMAH	Ethylamine	Putrescine	Cadaverine
10^{1}	+	–	+	+	+
10^{0}	–	–	+	+	+
10^{-1}	–	–	+	–	–
10^{-2}	–	–	–	–	–
10^{-3}	–	–	–	–	–
Reversibility	Reversible	–	Reversible	Irreversible	Irreversible

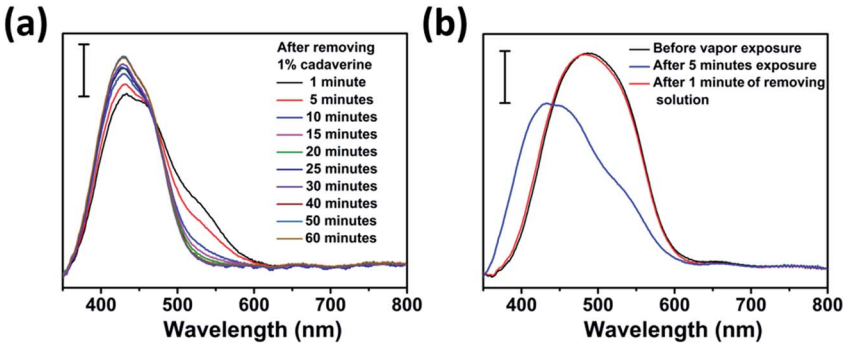

Fig. 2 Absorption spectra of dye sensor after removing the dye films from (a) ammonia and (b) cadaverine solutions. Note: due to the drift of calibration in the long measurement periods, the plotted curves were manually shifted vertically to set the intensity values equal at 800 nm. The vertical bars show 5% optical absorption.

effective resonance length of the delocalized electrons is shortened as the π-electrons of the carbonyl group are eliminated with the formation of the hemiaminal group resulting in a conjugated electron structure of higher energy.[31,32] We observe similar shift of the absorbance spectra for every other amine vapor except tetramethylammonium hydroxide (TMAH) (Fig. 1(b)). The lack of interaction in the latter case is due to the missing dative electron pair in the TMAH molecule that could attack on the highly positive carbon of the trifluoroacetyl group.

Interestingly, the reaction with the vapors of diamines such as putrescine and cadaverine appears to be irreversible (Table 1, and Fig. 2) or at least the reversed reaction is very slow. The reason of such behavior is related to a stabilization effect caused by the other amine group, which forms an intramolecular hydrogen bond with the hydroxyl group.[33] The reported rate constants for the product formation are considerably higher for the diamines than those for the corresponding monoamines. Also the equilibrium constants can be an order of magnitude higher when diamines take part in the formation of the carbinolamines, *i.e.* the reaction is shifted more towards the products with diamines than that with monoamines.[33] Based on ^{13}C-NMR spectroscopy data (see ESI†), the concentration of adducts in the reactant mixtures are also significantly higher for the diamines than for the monoamines (Table S1†) in qualitative agreement with the results of Mertz and co-workers.[33] The

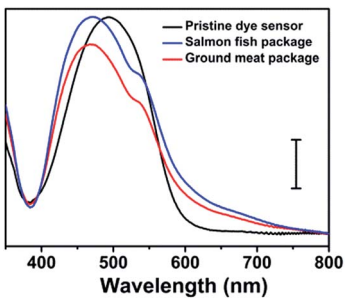

Fig. 4 Absorption spectra of dye sensors after 90 hours of storage in the presence of salted fish and grounded meat. The reference sensor was kept in a fume-hood for 90 hours. Note: due to the drift of calibration in the long measurement periods, the plotted curves were manually shifted vertically to set the intensity values equal at 800 nm. The vertical bar shows 5% optical absorption.

reaction of both amine groups of cadaverine with two trifluoroacetyl groups of 3-3′-di(trifluoroacetyl)-1,1′-bi-2-naphthol was proposed earlier[34] thus – in a similar way – we may also consider the formation of two hemiaminal groups with the participation of two dye molecules in the reaction resulting in dimers bridged by the diamines, which may also contribute to the better stability of the products.

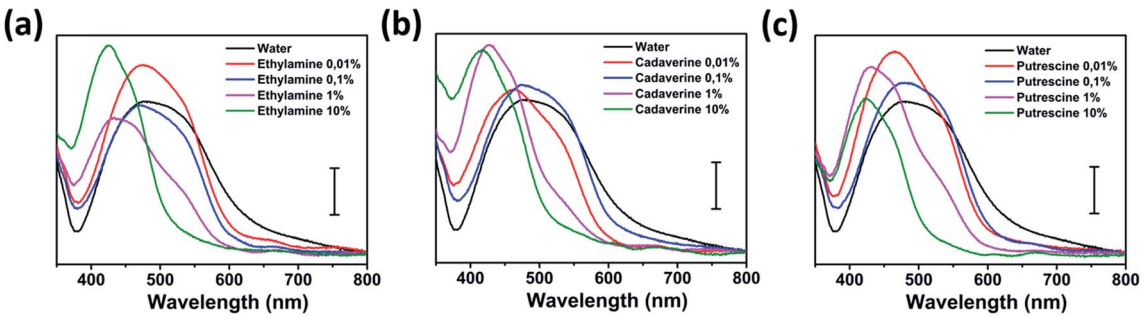

Fig. 3 Absorption spectra of dye sensor upon immersion into (a) ethylamine, (b) cadaverine and (c) putrescine solution. Note: due to the drift of calibration in the long measurement periods, the plotted curves were manually shifted vertically to set the intensity values equal at 800 nm. The vertical bars show 5% optical absorption.

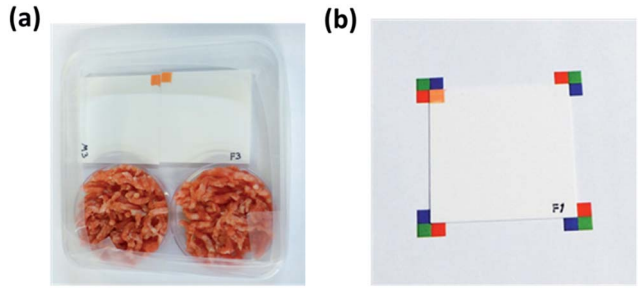

Fig. 5 Image of (a) food package, and (b) inkjet-printed dye sensor with reference color pattern.

Distinct recovering features of dye sensor after removing those from different amine solutions are observed. Rapid recovery happens in ammonia (Fig. 2(a)) and ethylamine (not shown) samples due to their high volatility. On the contrary, we found slight increase of absorbance of the shifted peak of dye molecule even after removing the sensors from the solutions of cadaverine (Fig. 2(b)) and putrescine (not shown). This latter effect may be explained by two processes. One is associated with the delayed reaction of physisorbed amines, while the other one is a rearrangement of hydrogen bonds established between the hemiaminal hydroxyl group and water molecules as well as non-bonding amine groups of diamines.

To further confirm the sensing limits of the optical dye sensors, measurements in the solution phase by immersing the dye sensor into different amine solutions were also performed. The acquired absorption spectra (Fig. 3) are almost the same as those assessed for the vapor phase experiments showing sensible amine concentrations from 0.1% or 1.0% (except TMAH, which is not shown here).

Since both putrescine and cadaverine are occurring in the degradation products of food (protein), it is plausible to test our sensors whether those are capable of indicating spoilage of *e.g.* meat and fish products. To examine the performance of the sensors in this context, dye films were placed in a glass container together with fresh meat as well as salmon (100 g each) after which the container was sealed. After 90 hours of storage in room temperature, a slight shift in the absorption spectra from 490 nm to 470 nm of the sensors was observed for both types of food samples (Fig. 4) as assessed by using spectrophotometer.

Table 3 Color shifts of dye sensors in Lab space after the exposure of food for 1 week along with the three reference colors in each image

Sample	$\lvert\overrightarrow{S_{blue}}\rvert$	$\lvert\overrightarrow{S_{red}}\rvert$	$\lvert\overrightarrow{S_{green}}\rvert$	$\lvert\overrightarrow{S_{food}}\rvert$
Meat #1	0.98	1.27	0.71	2.99
Meat #2	1.02	1.51	1.12	4.88
Fish #1	0.92	0.65	0.31	20.72
Fish #2	0.97	2.52	1.78	4.07

3.2 Color change analysis using digital camera and image processing of sensors in food packages

Although the color change of the dye films is clear when analyzing the samples with a spectrophotometer, in practical consumer friendly applications of the sensor, *e.g.* in a food package to detect spoilage of meat products, we need to visualize the changes with bare eyes or by using software-based automated analysis of digital camera images. The detection of color change by the identification of RGB, CMYK or Lab space coordinates is emerging today as feasible software based method applied on digital images.[35–37]

As the color change of the dye films was hardly detectable with our eyes, we acquired digital images using a photocamera and then analyzed the color of the images after converting the original RGB coordinates of the photographs to Lab color space using a built-in-function of MATLAB software (detail is described in ESI†).

To simulate the biogenic amine sensing for food package, the dye sensor was placed with ground meat and salmon fish in sealed plastic Petri dish respectively for one week (Fig. 5(a)). In addition, another printed dye sensor was kept in ambient condition for one week as the reference sample. For image acquisition, the exposed dye sensor was first placed next to printed red-green-blue color reference patterns (Fig. 5(b)) and three images were taken for each sample to eliminate the photographic difference in following image processing. After the color transformation from RGB space to Lab space, the color of reference blue-red-green pattern and dye sensor were digitalized as shown in Table 2. Each set of (L, a, b) numbers represents one color and was employed for further calculation and comparison.

Table 2 Quantification of reference color and sensor pattern in Lab space[a]

	Blue pattern			Red pattern			Green pattern			Sensor pattern		
Sample	L	a	b	L	a	b	L	a	b	L	a	b
Reference	18.26	9.49	−33.49	36.21	46.21	47.28	35.46	−24.80	27.92	49.75	30.84	39.29
Meat #1	19.02	8.94	−33.19	36.99	46.61	48.20	36.02	−24.62	28.31	51.48	29.48	41.32
Meat #2	18.99	9.96	−34.03	37.01	46.58	48.50	36.12	−24.99	28.81	50.90	31.29	44.01
Fish #1	18.73	9.74	−34.24	36.48	46.52	47.78	35.63	−24.71	28.16	57.21	16.70	26.11
Fish #2	19.03	9.74	−34.03	37.40	47.03	49.34	36.45	−25.20	29.34	51.14	31.16	43.10

[a] Color transformation from RGB space to Lab space is described in ESI.

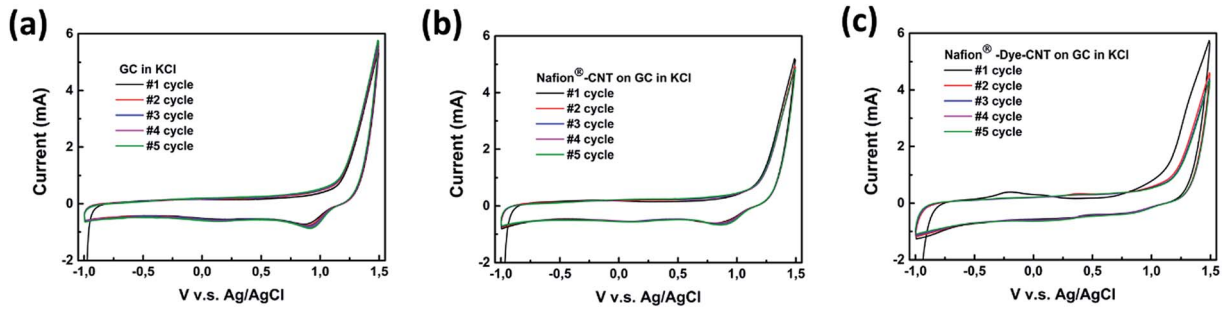

Fig. 6 Cyclic voltammograms of (a) glassy carbon (GC) electrode, (b) Nafion + CNT modified electrode and (c) dye + Nafion + CNT modified electrode in 0.1 M KCl. Scan rate used was 50 mV s^{-1} for each measurement and the voltammogram shown is from the first cycle if not otherwise indicated.

The color change of the dye sensor is expressed as a vector between the points belonging to reference and exposed samples in Lab color space (eqn (1)). To simplify the comparison of color change, we calculated the Euclidean distance of each vector (eqn (2)) as shown in Table 3.[37]

$$\left(L_{\text{sensor}} - L_{\text{ref}}, a_{\text{sensor}} - a_{\text{ref}}, b_{\text{sensor}} - b_{\text{ref}}\right) = \overrightarrow{S_{\text{sensor}}} \quad (1)$$

$$\sqrt{\left(L_{\text{sensor}} - L_{\text{ref}}\right)^2 + \left(a_{\text{sensor}} - a_{\text{ref}}\right)^2 + \left(b_{\text{sensor}} - b_{\text{ref}}\right)^2} = \left|\overrightarrow{S_{\text{sensor}}}\right| \quad (2)$$

Data in Table 3 clearly indicates the degree of color change of the dye sensors exceeds the photographic error in three reference color pattern $\left(\left|\overrightarrow{S_{\text{blue}}}\right|, \left|\overrightarrow{S_{\text{red}}}\right| \text{ and } \left|\overrightarrow{S_{\text{green}}}\right|\right)$. Note, in principle, the color change of these reference colors should be zero in each image. This result proves our established optical characterization procedure is feasible to detect the color change of the sensors in food packages without the employment of spectroscopy based analysis.

3.3 Electrochemical detection of amines using electrodes of dye–CNT–Nafion® composites

The results from the optical experiments on the detection of amines with the (trifluoroacetyl)azobenzene suggested to use the molecule to bond amines on the surface of electrode materials with the help of the dye. To explore this idea, we combined dye (the amine receptor), carbon nanotubes (conductive and porous electrode material with large surface area) and Nafion® (as electroactive polymer binder) and deposited the composite on the surface of glassy carbon electrodes. Although carbon nanotubes and Nafion® have been frequently used as electrode materials,[38] we expect to have an improved electrode performance owing to the amine sensitive

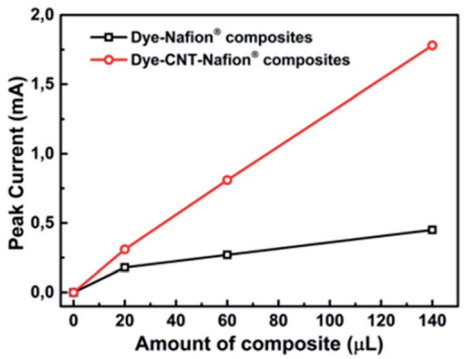

Fig. 8 Comparison of peak current corresponding to the electro-oxidation of cadaverine ($E_p \sim 0.8$ V *vs.* Ag/AgCl) shown in Fig. 7(b) and (c) after the background subtraction.

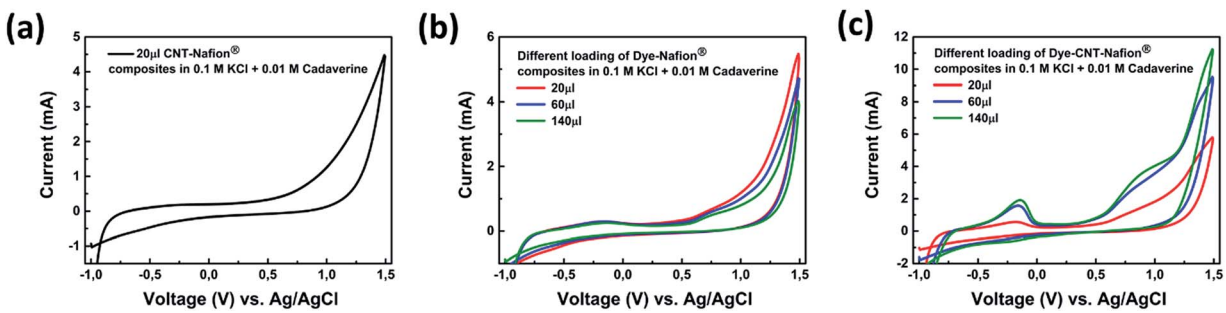

Fig. 7 Cyclic voltammetry curves of (a) Nafion®–CNT, (b) dye–Nafion® and (c) dye–Nafion–CNT composites in 0.1 M KCl electrolyte with the presence of 0.01 M cadaverine. The plots with different color compare the performance of composites with different amounts deposited on the glassy carbon electrode. The cycling speed used was 50 mV s^{-1} and all the voltammograms shown are from the first cycle.

Table 4 Increase in the peak current as a function of the amount of dye for dye–Nafion and dye–Nafion–CNT modified electrodes

Sample	Peak position (V *vs.* Ag/AgCl)	Peak current (mA)	Peak position (V *vs.* Ag/AgCl)	Peak current (mA)
Nafion®–dye 20 μL	−0.18	0.18	0.86	0.18
Nafion®–dye 60 μL	−0.18	0.16	0.88	0.27
Nafion®–dye 140 μL	−0.10	0.14	0.92	0.45
Nafion®–dye–CNT 20 μL	−0.21	0.30	0.83	0.31
Nafion®–dye–CNT 60 μL	−0.18	1.16	0.86	0.81
Nafion®–dye–CNT 140 μL	−0.17	1.47	0.89	1.78

molecule added to the electrode surface. To explore this, we used different electrode compositions and loadings with the composite to detect a diamine (cadaverine) by the means of cyclic-voltammetry.

Fig. 6(a)–(c) show series of voltammograms recorded for the different electrodes in KCl. As can be seen there is practically no difference between the voltammograms for the bare GC and Nafion + CNT modified electrodes. The capacitive background currents and the electrochemical windows are of the same order of magnitude. However, when the voltammogram of the dye–Nafion + CNT modified electrode is inspected it is evident that there are several differences in comparison to the previous two electrodes, which are expected to arise owing to the addition of the dye. The double layer charging current appears to be somewhat larger and it most likely contains also some faradic elements arising from different surface reactions. The latter is reflected in the fact that there is practically no flat double layer region in the voltammogram. More importantly, there is a clear oxidation peak around −0.2 V *vs.* (Ag/AgCl). This clearly indicates that the dye is oxidized during the anodic scan. The absence of any cathodic peaks during the reverse scan suggests that the electrochemical reaction step may be followed by a chemical reaction step that transforms the oxidized product into a non-electroactive form and can lead to partial or complete passivation of the electrode surface. This is further supported by the fact that subsequent scans shown in Fig. 6(c) are markedly different from the first scan and especially lack the oxidation peak at −0.2 V (*vs.* Ag/AgCl).

Next, the ability of the different electrode materials to detect cadaverine was investigated. Fig. 7(a)–(c) show a series of voltammograms where 0.01 M cadaverine has been added to KCl solution. As can be seen from Fig. 7(a) CNT + Nafion modified electrode appears to be insensitive to the presence of cadaverine in the solution. On the other hand when dye + Nafion modified electrode is used one can see a small peak around −0.2 V (*vs.* Ag/AgCl) corresponding to the oxidation of the dye itself (compare with Fig. 6(c)) as well as some rise in the oxidation current around 0.8 V (*vs.* Ag/AgCl). Based on the results it is clear that the magnitude of the measured current is not a function of the amount of dye + Nafion solution present on top of the electrode. Finally, when dye + Nafion + CNT modified electrodes are used one can see that there is a significant increase in the oxidation current around −0.2 V (*vs.* Ag/AgCl) as well as the appearance of a peak like feature around 0.8 V (*vs.* Ag/AgCl). The oxidation peak around −0.2 V (*vs.* Ag/AgCl), which is again due to the oxidation of the dye itself (see Fig. 6(c)) is much larger here suggesting that the carbinolamines – which form by the reaction of amines and the trifluoroacetylazobenzene dye – are more prone to oxidation. The oxidation peak that appears at ∼0.8 V is assigned to the oxidation of cadaverine similar to that reported for composite electrodes of β-cyclodextrin and sulfonated graphene oxide.[24] The magnitudes of the peak currents for both peaks are increased as the amount of dye + Nafion + CNT solution is increased (Fig. 8 and Table 4). Thus, it is evident that: (i) the presence of dye can promote oxidation of cadaverine, which takes place at around 0.8 V (*vs.* Ag/AgCl) as shown in Fig. 7(b) and (c) and that (ii) the presence of CNT network enhances the current response of the modified electrode, most likely by providing large surface area for adsorption of cadaverine as well as a percolating electrical network for more efficient charge transfer (Fig. 7(c)). The lack of any reduction peaks during the reverse scan again indicates that both oxidation processes are most likely followed by a chemical reaction step(s). This is supported also by the gradual deactivation/passivation of the electrode surfaces when repeated scans (not shown here) were carried out. Table 4 summarizes the results from the cadaverine measurements.

The CV curves measured for ammonium hydroxide, cadaverine, putrescine and their mixtures show rather similar features, *i.e.* the sensors cannot be considered as selective devices (Fig. S1†). It is worth mentioning, that the oxidation peak for the diamines is significantly stronger than that detected in ammonia solution. This result is coherent with the more pronounced product formation with the diamines than with monoamines.

4 Conclusions

Trifluoroacetylazobenzene dye films and dye–CNT–Nafion® composites are applied as amine sensor for optical and electrochemical detection of amines, respectively. The solution processed sensing materials were used in the forms of thin films. Spin coated dye films on PET substrates proved to be feasible for detecting various kinds of amines using optical spectroscopy for both vapors and solutions of the analytes. Similar but inkjet deposited thin films could be applied as miniaturized sensors for detecting the decomposition products of proteins – originating from meat and fish – using digital camera imaging and subsequent image processing. Furthermore, composites of the trifluoroacetylazobenzene

dye–CNT–Nafion® drop cast on glassy carbon electrodes were demonstrated as feasible materials to detect cadaverine by the means of cyclic voltammetry. Based on the results reported here, we envisage that after further optimization and selection of the sensing dye molecules, the demonstrated optical and electrochemical methods may serve as new approaches to detect or even quantify biogenic analytes having importance in environmental applications, food safety and medical analysis.

Author contributions

J.-F. L. prepared the samples and performed the optical and electrochemical measurements. Digital image acquisition and data processing were carried out by J. K. and T. S. NMR spectroscopy analysis was performed and evaluated by D. R. The experimental data were evaluated and discussed by every author. The manuscript was written by J.-F. L., T. L. and K. K. with the kind help of the coauthors.

Acknowledgements

The contributors acknowledge financial support received from projects Susfoflex (EU FP7), Prindemo_POC (Tekes), Autosys (Tekes) and Infotech Oulu.

References

1 C. McDonagh, C. S. Burke and B. D. MacCraith, *Chem. Rev.*, 2008, **108**, 400–422.
2 H. H. Qazi, A. B. B. Mohammad and M. Akram, *Sensors*, 2012, **12**, 16522–16556.
3 T. Tran-Thi, R. Dagnelie, S. Crunaire and L. Nicole, *Chem. Soc. Rev.*, 2011, **40**, 621–639.
4 V. C. Gonçalves and D. T. Balogh, *Sens. Actuators, B*, 2012, **162**, 307–312.
5 T. L. Nelson, C. O'Sullivan, N. T. Greene, M. S. Maynor and J. J. Lavigne, *J. Am. Chem. Soc.*, 2006, **128**, 5640–5641.
6 J. Wu, X. Lu, F. Shan, J. Guan and Q. Lu, *RSC Adv.*, 2013, **3**, 22841–22844.
7 L. I. Silva, A. C. Freitas, T. A. Rocha-Santos, M. E. Pereira and A. C. Duarte, *Talanta*, 2011, **83**, 1586–1594.
8 S. Goswami, S. Paul and A. Manna, *RSC Adv.*, 2013, **3**, 18872–18877.
9 W. Shi, S. He, M. Wei, D. G. Evans and X. Duan, *Adv. Funct. Mater.*, 2010, **20**, 3856–3863.
10 W. Wei, X. Huang, K. Chen, Y. Tao and X. Tang, *RSC Adv.*, 2012, **2**, 3765–3771.
11 K. Secor, J. Plante, C. Avetta and T. Glass, *J. Mater. Chem.*, 2005, **15**, 4073–4077.
12 J. Homola, S. S. Yee and G. Gauglitz, *Sens. Actuators, B*, 1999, **54**, 3–15.
13 H. A. Azab, S. A. El-Korashy, Z. M. Anwar, G. M. Khairy and A. Duerkop, *J. Photochem. Photobiol., A*, 2012, **243**, 41–46.
14 K. W. Bentley, Y. G. Nam, J. M. Murphy and C. Wolf, *J. Am. Chem. Soc.*, 2013, **135**, 18052–18055.
15 T. Minami, N. A. Esipenko, A. Akdeniz, B. Zhang, L. Isaacs and P. Anzenbacher Jr, *J. Am. Chem. Soc.*, 2013, **135**, 15238–15243.
16 A. Pacquit, J. Frisby, D. Diamond, K. T. Lau, A. Farrell, B. Quilty and D. Diamond, *Food Chem.*, 2007, **102**, 466–470.
17 H. Kwon, F. Samain and E. T. Kool, *Chem. Sci.*, 2012, **3**, 2542–2549.
18 G. J. Mohr, *Chem.–Eur. J.*, 2004, **10**, 1082–1090.
19 G. J. Mohr, *Anal. Chim. Acta*, 2004, **508**, 233–237.
20 S. Reinert and G. J. Mohr, *Chem. Commun.*, 2008, 2272–2274.
21 N. Kirchner, L. Zedler, T. G. Mayerhöfer and G. J. Mohr, *Chem. Commun.*, 2006, 1512–1514.
22 J. H. T. Luong, S. Hrapovic and D. S. Wang, *Electroanalysis*, 2005, **17**, 47–53.
23 B. E. K. Swamy and B. J. Venton, *Analyst*, 2007, **132**, 876–884.
24 L. Saghatforoush, M. Hasanzadeh and N. Shadjou, *J. Electroanal. Chem.*, 2014, **714**, 79–84.
25 M. L. Rodriguez-Mendez, M. Gay, C. Apetrei and J. A. De Saja, *Electrochim. Acta*, 2009, **54**, 7033–7041.
26 A. Ferancova, E. Korgova, J. Labuda, J. Zima and J. Barek, *Electroanalysis*, 2002, **14**, 1668–1673.
27 S. Shahrokhian and H. R. Zare-Mehrjardi, *Electrochim. Acta*, 2007, **52**, 6310–6317.
28 A. Liu, I. Honma and H. Zhou, *Biosens. Bioelectron.*, 2007, **23**, 74–80.
29 U. Yogeswaran, S. Thiagarajan and S. M. Chen, *Anal. Biochem.*, 2007, **365**, 122–131.
30 Z. Dursun and B. Gelmez, *Electroanalysis*, 2010, **22**, 1106–1114.
31 B. E. Kohler and I. D. W. Samuel, *J. Chem. Phys.*, 1995, **103**, 6248–6252.
32 H. Meier, U. Stalmach and H. Kolshorn, *Acta Polym.*, 1997, **48**, 379–384.
33 E. Mertz, J. B. Beil and S. C. Zimmerman, *Org. Lett.*, 2003, **5**, 3127–3130.
34 S. Yu, W. Plunkett, M. Kim, E. Wu, M. Sabat and L. Pu, *J. Org. Chem.*, 2013, **78**, 12671–12680.
35 E. A. Davey, A. J. Zucchero, O. Trapp and U. H. F. Bunz, *J. Am. Chem. Soc.*, 2011, **133**, 7716–7718.
36 N. A. Rakow and K. S. Suslick, *Nature*, 2000, **406**, 710–713.
37 S. Westland, C. Ripamonti and V. Cheung, *CIELAB and Colour Difference, in Computational Colour Science using MATLAB®*, 2nd edn, 2012, ch. 5.
38 Y.-C. Tsai, J.-M. Chen, S.-C. Li and F. Marken, *Electrochem. Commun.*, 2004, **6**, 917.

